L. P. Hunter

Direct Measurement of the Angular Dependence of the Imaginary Part of the Atomic Scattering Factor of Germanium

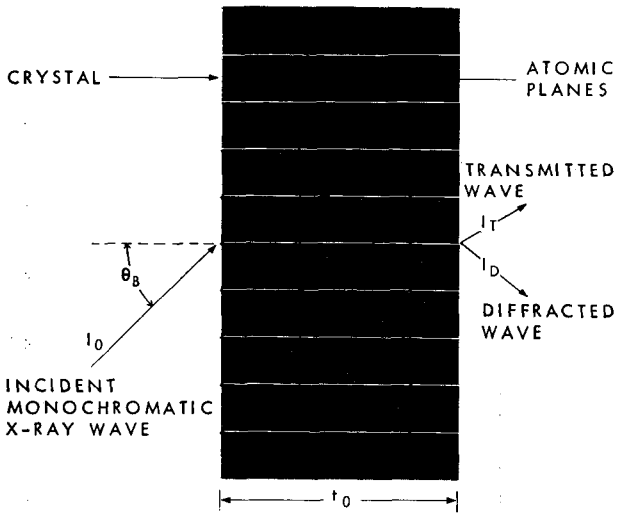

Abstract: In the dynamical theory of the anomalous transmission of x-rays through perfect thick crystals, the ratio of transmitted intensity to incident intensity depends upon $[1-Kf''_{Ge}(\theta_{hkl})/f''_{Ge}(0°)]$ exponentially. Here K is the polarization factor and the $f''_{Ge}(\theta_{hkl})$ and $f''_{Ge}(0°)$ are the imaginary parts of the atomic scattering factors of germanium at the angle θ_{hkl} and 0°, respectively. This paper describes the measurement of the ratio $f''_{Ge}(\theta_{hkl})/f''_{Ge}(0°)$ for several different sets of planes in nearly perfect germanium crystals.

Figure 1 **The anomalous transmission of x-rays.**

Introduction

The anomalous transmission of x-rays through nearly perfect thick crystals was first observed by Borrmann[1] and Campbell[2] and has been discussed theoretically by Hirsch,[3] von Laue,[4] Zachariasen[5] and Kato,[6] and investigated experimentally by Schwartz and Rogosa.[7] A brief note has been published by the author[8] outlining several experiments using anomalous transmission of x-rays, including the experiment described in detail in this paper.

The intensity of the anomalous transmission of x-rays depends upon the degree of crystalline perfection of the sample used, as well as upon the geometry of the electronic structure of the crystal. It is necessary to use the most perfect crystals obtainable and then to correct the results for the residual imperfections if one wishes to measure the imaginary part of the atomic scattering factor.

In recent times germanium single crystals of a very high degree of perfection have become available.[9] These crystals show no dislocations, as revealed by etching techniques.[10] They do show evidence of other imperfections, but it is possible to correct the transmitted intensity measurements for these. The purpose of this paper is to discuss the direct measurement of the angular dependence of the imaginary part of the atomic scattering factor using the anomalous transmission of x-rays through nearly perfect thick crystals. The results obtained on germanium will be given in some detail.

Theory

The anomalous transmission of x-rays can best be understood physically by reference to Fig. 1. If the x-rays are monochromatic and incident at the Bragg angle, θ_B, there will result multiple reflections between the atomic planes of the crystal. Because of these multiple reflections, we can resolve the incident x-ray traveling wave into two standing-wave components; A, with the nodes of its electric field coincident in position with the family of atomic planes (hkl) and, B, with the nodes of its electric field elsewhere. As we proceed into the crystal it is clear that B will be attenuated much more rapidly than A, and if the crystal is sufficiently thick, only the standing wave A will reach the opposite face. In this case standing wave A alone will be resolved into two traveling waves making equal angles θ_B with the atomic planes of the crystal. One

L. P. Hunter

Direct Measurement of the Angular Dependence of the Imaginary Part of the Atomic Scattering Factor of Germanium

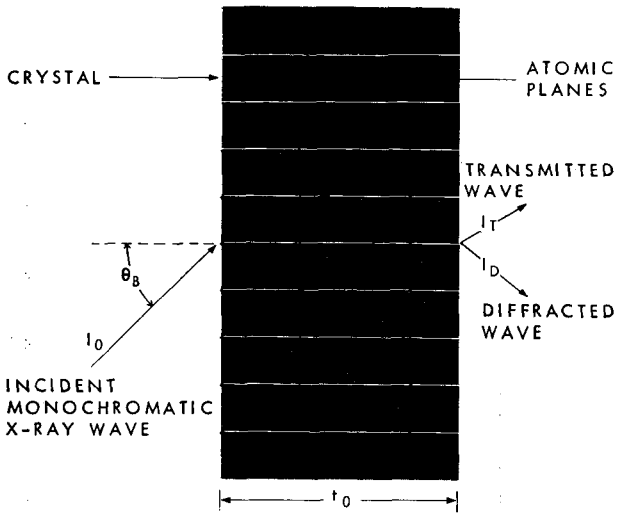

Abstract: In the dynamical theory of the anomalous transmission of x-rays through perfect thick crystals, the ratio of transmitted intensity to incident intensity depends upon $[1-Kf''_{Ge}(\theta_{hkl})/f''_{Ge}(0°)]$ exponentially. Here K is the polarization factor and the $f''_{Ge}(\theta_{hkl})$ and $f''_{Ge}(0°)$ are the imaginary parts of the atomic scattering factors of germanium at the angle θ_{hkl} and 0°, respectively. This paper describes the measurement of the ratio $f''_{Ge}(\theta_{hkl})/f''_{Ge}(0°)$ for several different sets of planes in nearly perfect germanium crystals.

Figure 1 **The anomalous transmission of x-rays.**

Introduction

The anomalous transmission of x-rays through nearly perfect thick crystals was first observed by Borrmann[1] and Campbell[2] and has been discussed theoretically by Hirsch,[3] von Laue,[4] Zachariasen[5] and Kato,[6] and investigated experimentally by Schwartz and Rogosa.[7] A brief note has been published by the author[8] outlining several experiments using anomalous transmission of x-rays, including the experiment described in detail in this paper.

The intensity of the anomalous transmission of x-rays depends upon the degree of crystalline perfection of the sample used, as well as upon the geometry of the electronic structure of the crystal. It is necessary to use the most perfect crystals obtainable and then to correct the results for the residual imperfections if one wishes to measure the imaginary part of the atomic scattering factor.

In recent times germanium single crystals of a very high degree of perfection have become available.[9] These crystals show no dislocations, as revealed by etching techniques.[10] They do show evidence of other imperfections, but it is possible to correct the transmitted intensity measurements for these. The purpose of this paper is to discuss the direct measurement of the angular dependence of the imaginary part of the atomic scattering factor using the anomalous transmission of x-rays through nearly perfect thick crystals. The results obtained on germanium will be given in some detail.

Theory

The anomalous transmission of x-rays can best be understood physically by reference to Fig. 1. If the x-rays are monochromatic and incident at the Bragg angle, θ_B, there will result multiple reflections between the atomic planes of the crystal. Because of these multiple reflections, we can resolve the incident x-ray traveling wave into two standing-wave components; A, with the nodes of its electric field coincident in position with the family of atomic planes (hkl) and, B, with the nodes of its electric field elsewhere. As we proceed into the crystal it is clear that B will be attenuated much more rapidly than A, and if the crystal is sufficiently thick, only the standing wave A will reach the opposite face. In this case standing wave A alone will be resolved into two traveling waves making equal angles θ_B with the atomic planes of the crystal. One

traveling wave will be parallel to the incident wave I_0 and will be called the transmitted wave of intensity I_T. The other wave will make an angle of $2\theta_B$ with the incident wave and will be called the diffracted wave with intensity I_D. From symmetry considerations, it is clear that if the standing wave B is completely absorbed, the resolution of standing wave A will give $I_T=I_D$. If the atoms of the crystal are at rest in perfect planes, and if, in addition, the atoms are point atoms in the sense that there will be no photoelectric absorption of x-rays by the atoms if there is zero electric field at the atom center, there will be no absorption of standing wave A as it passes through the crystal. The consequence of this is that $I_T=I_D=I_0/4$ regardless of the thickness of the crystal, as long as it is thick enough to completely absorb standing wave B.

To calculate the quantitative formulas which apply to real crystals we will follow Hirsch,[3] whose Eqs. (11) and (12) are reproduced below for the symmetrical Laue reflection:

$$\frac{I_D}{I_0}=\frac{1}{2}\frac{\exp(-\mu_0 t)}{(1+y^2)}\cosh\frac{\mu_0 t\varepsilon}{\sqrt{1+y^2}}$$

$$\frac{I_T}{I_0}=\frac{1}{2}\frac{\exp(-\mu_0 t)}{(1+y^2)}\cosh\left(\frac{\mu_0 t\varepsilon}{\sqrt{1+y^2}}\pm X\right), \qquad (1)$$

where

μ_0 is the linear absorption coefficient of the x-rays used.

t is the thickness of the crystal in the direction of the x-ray beam.

$\varepsilon=K(F''_{hkl}/F''_{000})$.

K is the polarization factor (unity or $\cos 2\theta$ for x-rays with the electric vector perpendicular or parallel to the plane of incidence of the x-rays).

F''_{hkl} is the imaginary part of the crystalline structure factor for the (hkl) reflection (I_D).

F''_{000} is the imaginary part of the crystalline structure factor for the directly transmitted beam (I_T).

$y=(\theta_B-\theta)(\sin 2\theta_B)/CKF_{hkl}$.

$C=4\pi e^2/m\omega_0^2 V$, where e and m are the charge and mass of the electron, ω_0 is 2π times the frequency of the x-rays, and V is the volume of the unit cell of the crystal.

F_{hkl} is the crystalline structure factor for the (hkl) reflection.

$\cosh X=1+2y^2$ and the sign of X is the same as the sign of y.

The equations (1) are valid over the entire range of crystal thicknesses from $t=0$ to ∞. They are valid for finite atoms but do assume that the atoms are at rest in perfect planes. For our application we will be concerned only with thick crystals. Here we will define thick crystals to have $\mu_0 t>10$. By making the thick-crystal approximation we can considerably simplify the equations (1). First expanding the cosh in terms of exponentials, we may write equations (1) in the form:

$$\frac{I_D}{I_0}=\frac{\exp[-\mu_0 t(1-\varepsilon/\sqrt{1+y^2})]}{4(1+y^2)}+\frac{\exp[-\mu_0 t(1+\varepsilon/\sqrt{1+y^2})]}{4(1+y^2)}$$

$$\frac{I_T}{I_0}=\frac{\exp[-\mu_0 t(1-\varepsilon/\sqrt{1+y^2})]}{4(1+y^2)}\times\{(1+2y^2)-2y\sqrt{1+y^2}\}+\frac{\exp[-\mu_0 t(1+\varepsilon/\sqrt{1+y^2})]}{4(1+y^2)}\times\{(1+2y^2)+2y\sqrt{1+y^2}\}. \qquad (2)$$

It turns out experimentally that $0.75<\varepsilon<1.00$ for all of the reflections considered here, so we may neglect the second terms of the equations (2) compared to the first terms for the thick-crystal case. This leaves us:

$$\frac{I_D}{I_0}=\frac{\exp[-\mu_0 t(1-\varepsilon/\sqrt{1+y^2})]}{4(1+y^2)}$$

$$\frac{I_T}{I_0}=\frac{\exp[-\mu_0 t(1-\varepsilon/\sqrt{1+y^2})]}{4(1+y^2)}\times\{(1+2y^2)-2y\sqrt{1+y^2}\}. \qquad (3)$$

Careful examination of the equations (3) shows that for large values of $\mu_0 t$ the exponential term varies much faster than the algebraic factors. This means that, for all practical purposes, for thick crystals we may consider that

$$\frac{I_T}{I_0}=\frac{I_D}{I_0}=\frac{1}{4}\exp[-\mu_0 t(1-\varepsilon/\sqrt{1+y^2})]. \qquad (4)$$

In Fig. 2 is shown a comparison of I_T/I_0, I_D/I_0, and $(1/4)\exp[-\mu_0 t(1-\varepsilon/\sqrt{1+y^2})]$ plotted against y for $\mu_0 t=10$ and $\varepsilon=0.9$. This comparison shows that the curve of Eq. (4) encloses an area intermediate between the curves of I_T/I_0 and I_D/I_0. Numerical integration over y for these curves yields the values shown in the table of Fig. 2. These integrated values are proportional to the integrated intensities we will measure in the experiments described in this paper, and the values of $\int(I_T/I_0)dy$ and $\int(I_D/I_0)dy$ are seen to differ less than 10% from the value of the integral of Eq. (4). If the same comparison is made at $\mu_0 t=20$, the deviation of the same values is less than 5%. In view of this we will proceed on the basis that the integrated intensity of either the transmitted or diffracted beam is adequately represented by the integral of Eq. (4) for crystals with $\mu_0 t>10$.

To integrate Eq. (4) we write it in the approximate form:

$$\frac{I_T}{I_0}=\frac{I_D}{I_0}=\tfrac{1}{4}\exp(-\mu_0 t)\exp[\varepsilon\mu_0 t/(1+\tfrac{1}{2}y^2)]$$
$$=\tfrac{1}{4}\exp(-\mu_0 t)\exp(\varepsilon\mu_0 t)\exp(-\tfrac{1}{2}\varepsilon\mu_0 t y^2). \qquad (5)$$

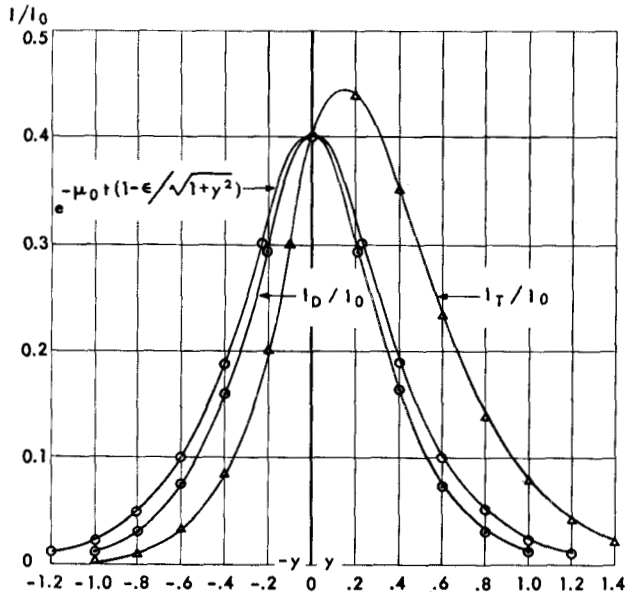

Numerically integrated intensities

I_T/I_0	$=0.102$
I_D/I_0	$=0.080$
$\exp[-\mu_0 t(1-\varepsilon/\sqrt{1+y^2})]$	$=0.091$

Figure 2 **Calculated intensity curves using $\varepsilon=0.90$ and $\mu_0 t=10$.**

This approximation assumes that y^2 is small compared to unity over the range of rapid variation of the exponential. Integrating, we get:

$$R_T^y = R_D^y = \tfrac{1}{4}\exp[-\mu_0 t(1-\varepsilon)]\int_{-\infty}^{+\infty}\exp(-\tfrac{1}{2}\varepsilon\mu_0 t y^2)\,dy$$

$$= \sqrt{\pi/8\varepsilon\mu_0 t}\exp[-\mu_0 t(1-\varepsilon)]\,. \qquad (6)$$

This approximate result is good to 10% for all values of $\mu_0 t$ in excess of 20 and values of $\varepsilon>0.75$. If it is desired to calculate the integrated intensities for values of $\mu_0 t$ and ε lower than these, it must be done numerically.

Equation (6) gives the ratio of the sum of the intensities at all values of y to the incident monochromatic x-ray intensity. It should be pointed out that Eq. (6) really represents two equations, one for the parallel polarization component of the incident x-rays and a second for the perpendicular component. Writing Eq. (6) to bring this out, we have:

$$^{\perp}R_T^y = {}^{\perp}R_D^y = \left(\frac{\pi}{8\mu_0 t}\frac{F''_{000}}{F''_{hkl}}\right)^{1/2}\exp\left[-\mu_0 t\left(1-\frac{F''_{hkl}}{F''_{000}}\right)\right] \qquad (6a)$$

$$^{\parallel}R_T^y = {}^{\parallel}R_D^y = \left(\frac{\pi}{8\mu_0 t\cos 2\theta_B}\frac{F''_{000}}{F''_{hkl}}\right)^{1/2}$$

$$\exp\left[-\mu_0 t\left(1-\frac{F''_{hkl}}{F''_{000}}\cos 2\theta_B\right)\right]. \qquad (6b)$$

In order to develop these equations for use, we must consider them in connection with the actual method we will use to measure integrated intensity experimentally. This method consists of collimating the x-rays to a narrow beam of about 40 seconds divergence and reflecting the beam from a monochromator crystal. After leaving the monochromator crystal, the $K\alpha_2$ line is suppressed by a slit system, leaving the monochromatic $K\alpha_1$ line to fall on the surface of the sample crystal. The intensity of this line in x-ray photons per sec is the I_0 referred to above. The sample crystal is now rotated at a uniform angular speed ω through the angle θ_B and over a range somewhat greater than the natural width of the transmitted-intensity curve (Fig. 2) plus the angular divergence of the incident beam. The total number of x-ray photons received behind the sample during the entire crystal rotation minus the background is the integrated intensity measured.

The integration over y represented by the equations (6) must be corrected to give the equivalent sum over θ and the effect of the monochromator crystal must be evaluated. No special integration over the divergency of the beam is necessary because each ray of the beam can be considered as merely requiring a slightly different crystal setting of the sample; and as long as our rotation is over an angle greater than the divergency of the beam, we will be utilizing the full intensity of the beam to exactly the same degree as if all the rays were parallel and we rotated over an angle just sufficient to include the natural angular width of the transmitted line.

From the definition of y we are able to relate the integrations over y (R_T^y and R_D^y) to corresponding integrations over θ (R_T^θ and R_D^θ). These relations are given below:

$$R_T^\theta = R_D^\theta = \frac{CKF_{hkl}}{\sin 2\theta_B}R_T^y\,, \qquad (7)$$

and in terms of two different polarization directions we have:

$$^{\perp}R_T^\theta = {}^{\perp}R_D^\theta = \frac{CF_{hkl}}{\sin 2\theta_B}\left(\frac{\pi}{8\mu_0 t}\frac{F''_{000}}{F''_{hkl}}\right)^{1/2}$$

$$\exp\left[-\mu_0 t\left(1-\frac{F''_{hkl}}{F''_{000}}\right)\right] \qquad (7a)$$

$$^{\parallel}R_T^\theta = {}^{\parallel}R_D^\theta = \frac{CF_{hkl}\cos 2\theta_B}{\sin 2\theta_B}\left(\frac{\pi}{8\mu_0 t\cos 2\theta_B}\frac{F''_{000}}{F''_{hkl}}\right)^{1/2}$$

$$\exp\left[-\mu_0 t\left(1-\frac{F''_{hkl}}{F''_{000}}\cos 2\theta_B\right)\right]. \qquad (7b)$$

If we now assume that the x-ray beam leaving the monochromator crystal and incident upon the sample crystal is practically unpolarized, the total integrated intensity will be given by the average of Eqs. (7a) and (7b). This assumption is good for the quartz monochromator used since the diffracting angle from the quartz was only 13.2°, and this gives only about 5% polarization. The total integrated intensity, R, transmitted by the crystal in either the transmitted or diffracted beam is given by the average:

$$R=\tfrac{1}{2}({}^{\perp}R_T^{\theta}+{}^{\parallel}R_T^{\theta})=\frac{CF_{hkl}}{\sin 2\theta_B}\left(\frac{\pi}{8\mu_0 t}\frac{F''_{000}}{F''_{hkl}}\right)^{1/2}$$
$$\times\frac{1}{2}\left\{\exp\left[-\mu_0 t\left(1-\frac{F''_{hkl}}{F''_{000}}\right)\right]\right.$$
$$\left.+(\cos^{1/2}2\theta_B)\exp\left[-\mu_0 t\left(1-\frac{F''_{hkl}}{F''_{000}}\cos 2\theta_B\right)\right]\right\}. \quad (8)$$

If the sample crystal is rotated at angular speed ω, the experimentally determined total x-ray count, E, is related to R by the relation:

$$\frac{E_\omega}{I_0}=R\,, \quad (9)$$

where I_0 is the intensity of the monochromatic beam striking the sample crystal.

Combining Eqs. (8) and (9) we find the following relation:

$$\frac{\ln(I_0/\omega E)}{\mu_0 t}=\left(1-\frac{F''_{hkl}}{F''_{000}}\right)+\left\{\ln\frac{2\sin 2\theta_B}{CF_{hkl}}\right.$$
$$+\frac{1}{2}\ln\left(\frac{8\mu_0 t}{\pi}\frac{F''_{hkl}}{F''_{000}}\right)-\ln\left[1+(\cos^{1/2}2\theta_B)\right.$$
$$\left.\left.\exp\left(-\mu_0 t\frac{F''_{hkl}}{F''_{000}}(1-\cos 2\theta_B)\right)\right]\right\}\Big/\mu_0 t\,. \quad (10)$$

Examination of Eq. (10) shows that the last logarithmic term is negligible compared to the others for $\mu_0 t>10$.*

The ratio F''_{hkl}/F''_{000} of the imaginary parts of the crystalline structure factors can be expressed as the ratio $f''_{Ge}(\theta_B)/f''_{Ge}(0°)$ of the imaginary parts of the atomic scattering factor of germanium for the particular measurements described in this paper. This may be demonstrated from the fact that the germanium crystal lattice possesses a center of symmetry. The definition of the crystalline structure factor is given by:

$$F_{hkl}=\sum_j f_j\exp(2\pi i\bar{B}_{hkl}\bar{r}_j)\,, \quad (11)$$

where f_j is the atomic scattering factor for the j^{th} atom in the unit cell of the crystal, $\bar{B}_{hkl}$ is the reciprocal lattice vector for the crystal planes (hkl), and $\bar{r}_j$ is the vector from the origin to the j^{th} atom in the unit cell.

In a crystal of germanium there are eight germanium atoms per unit cell. All of the f_j's, therefore, equal the atomic scattering factor of germanium, f_{Ge}. The atoms of the germanium crystal are arranged in two interpenetrating fcc lattices which are separated by the coordinates $(\frac{1}{4}\,\frac{1}{4}\,\frac{1}{4})$. Such a system obviously has a center of symmetry at the position $(\frac{1}{8}\,\frac{1}{8}\,\frac{1}{8})$. (The coordinates are expressed in fractions of a unit-cell edge.) If the coordinates of the eight atoms of the unit cell are substituted into Eq. (11), it will be seen that the imaginary parts of F_{hkl} vanish for all values of (hkl) for this symmetry of atomic coordinates, leaving the only remaining source of an imaginary component as the f_{Ge} itself.

*This is equivalent to ${}^{\parallel}R^{\theta}\to 0$ because of $\cos 2\theta_B$ dependence in the exponential term.

By calculation it is readily found that all atomic planes with odd (hkl) values give $|F_{hkl}|=8f_{Ge}/\sqrt{2}$; all planes with even (hkl) values where the sum $h+k+l$ is a multiple of 4 give $|F_{hkl}|=8f_{Ge}$; and all other planes give $|F_{hkl}|=0$. From this it is clear that the ratio (F''_{hkl}/F''_{000}) becomes $0.707[f''_{Ge}(\theta_{hkl})/f''_{Ge}(0°)]$ for reflections from atomic planes with odd (hkl) values and becomes $1.00[f''_{Ge}(\theta_{hkl})/f''_{Ge}(0°)]$ for reflections from atomic planes with even (hkl) values whose sum is a multiple of 4. Since the intensity of the anomalous transmission depends quite strongly on minimizing the quantity $(1-F''_{hkl}/F''_{000})$, we must use reflections with even (hkl) values so that the ratio (F''_{hkl}/F''_{000}) is as large as possible. Accordingly we may rewrite Eq. (10), dropping negligible terms and substituting for the ratio (F''_{hkl}/F''_{000}),

$$\frac{\ln(I_0/\omega E)}{\mu_0 t}=\left(1-\frac{f''_{Ge}(\theta_B)}{f''_{Ge}(0°)}\right)+\left\{\ln\frac{2\sin 2\theta_B}{C8f_{Ge}}\right.$$
$$\left.+\frac{1}{2}\ln\left(\frac{8\mu_0 t}{\pi}\frac{f''_{Ge}(\theta_B)}{f''_{Ge}(0°)}\right)\right\}\Big/\mu_0 t\,. \quad (12)$$

Equation (12) is the final equation we will use for the reduction of the experimental measurements. Examination of this equation shows that a plot of the left-hand side against the second term on the right-hand side will, to the first approximation, yield a 45-degree line with an intercept on the ordinate equal to the quantity $[1-f''_{Ge}(\theta_B)/f''_{Ge}(0°)]$. If this quantity is determined for several different reflections (different values of θ_B), we will have achieved our goal of the direct measurement of the angular dependence of the imaginary part of the atomic scattering factor of germanium.

Experiment

The experimental arrangement is shown in Fig. 3. The x-ray source was a standard Philips x-ray generator with a standard Philips copper tube. The focal spot is nominally 1 mm × 10 mm and the takeoff angle was about 6° in a plane perpendicular to the long axis of the focal spot. This gives an effective projected line source of about 0.1 mm × 10 mm. The collimating slits were 0.1 mm × 1 mm. The monochromator crystal was quartz cut to reflect from the (101) planes. The exit slit was also 0.1 mm × 1 mm and was set to eliminate the Cu$K\alpha_2$ radiation. The germanium crystal sample was mounted at the center of rotation of a spectrometer on traverse screws so that the crystal might be scanned both vertically and horizontally while still keeping the axis of rotation in the crystal and parallel to the reflecting planes. A motor-driven micrometer was placed against the end of a long lever arm and was used to rotate the crystal through its diffracting position. The angular position of the occurrence of the peak transmission could be read on the micrometer.

The x-ray detector used was a proportional counter with a pulse-height discriminator circuit, so that the higher harmonics coming through the monochromator would not be counted. A check was made for the presence of higher harmonics by using different combinations of

voltage and current on the x-ray tube to see if the ratio I_T/I_0 were higher for the higher voltage settings. Since no effect was found, it was concluded that no significant intensity of higher harmonics was being counted.

The initial samples used for the measurements were cut wedge-shaped, with the diffracting planes perpendicular to the direction of taper of the wedge. The wedges were mounted so that the long dimension of the x-ray beam was parallel to the crystal planes. The crystal translations mentioned above provided the ability to scan along the length of the wedge without changing its angle to the x-ray beam and maintaining the axis of rotation within the crystal. A typical wedge was 20 mm long, 3 mm wide and tapered from a thickness of about 0.5 mm to 1.5 mm.

A study was made of the effects of surface damage due to grinding the sample to shape. It was found that the anomalous transmission measured on a 1-mm sample, ground to shape and lapped with 1200-mesh abrasive to remove all grinding scratches, was only about 5% of the transmission measured after a heavy CP4 etch. (This percentage includes correction for the reduced thickness.) Experimentation showed that if 20 microns or more were removed by etching from the surfaces through which the x-rays pass, there was no reduction of the anomalous transmission by surface damage.

The measurement of I_0 was achieved by using the thin end of the sample crystal wedge as a filter. The x-ray tube was first set at a current and voltage within the regulating range of the x-ray generator and yet at a sufficiently low level that the proportional counter could measure the direct beam from the monochromator. At this setting of current and voltage both the direct beam and the integrated intensity through the thin end of the crystal wedge were measured. The x-ray generator was now set at the usual operating current and voltage, and the integrated intensity was again measured through the same point on the crystal wedge, thus providing a calibrating factor.

In order to use the equations developed above, we must know the μ_0 of single-crystal germanium for the wavelengths of the x-rays to be used. Even though values of μ_0 are to be found in the literature it was felt desirable to measure it directly. For this purpose a slab of germanium single crystal was lapped and etched to a thickness of 0.210 mm. The normal transmission of the monochromatic x-rays was measured through this slab for several different angles of incidence of the x-rays. Since this slab was taken from a good single crystal it was possible to use the anomalous transmission method of determining I_0 as described above. The normal transmissions at the various angular settings were corrected for the cosine of the angle, and the resulting values of I_T/I_0 were averaged to yield $\mu_0 = 326$ per cm for Cu$K\alpha_1$ radiation.

Wedge samples were used to determine the value of $[1-f''_{Ge}(\theta_B)/f''_{Ge}(0°)]$ for the (220) and (400) reflections by the extrapolation method described in the discussion of Eq. (12). The plotting of Eq. (12), as described, requires only that we have measured the anomalous transmission as a function of $\mu_0 t$. Since scanning our wedge-shaped samples provides a variation in t, we can get enough data from one wedge sample to give a complete determination of $[1-f''_{Ge}(\theta_B)/f''_{Ge}(0°)]$ for one reflection.

For higher-order reflections wedge samples were not used, because the reduced anomalous transmission of the higher orders will not allow sufficiently large values of t to be measured to give a good extrapolation to $t=\infty$. To measure the higher-order reflections, samples were prepared in the form of flat discs of uniform thickness and oriented so that the [110] crystallographic direction is perpendicular to the plane of the disc. A disc oriented in this way has the [100], [110] and [112] crystallographic directions at different azimuths in the plane of the disc.

Figure 3 **Schematic arrangement of apparatus for anomalous-transmission measurement.**

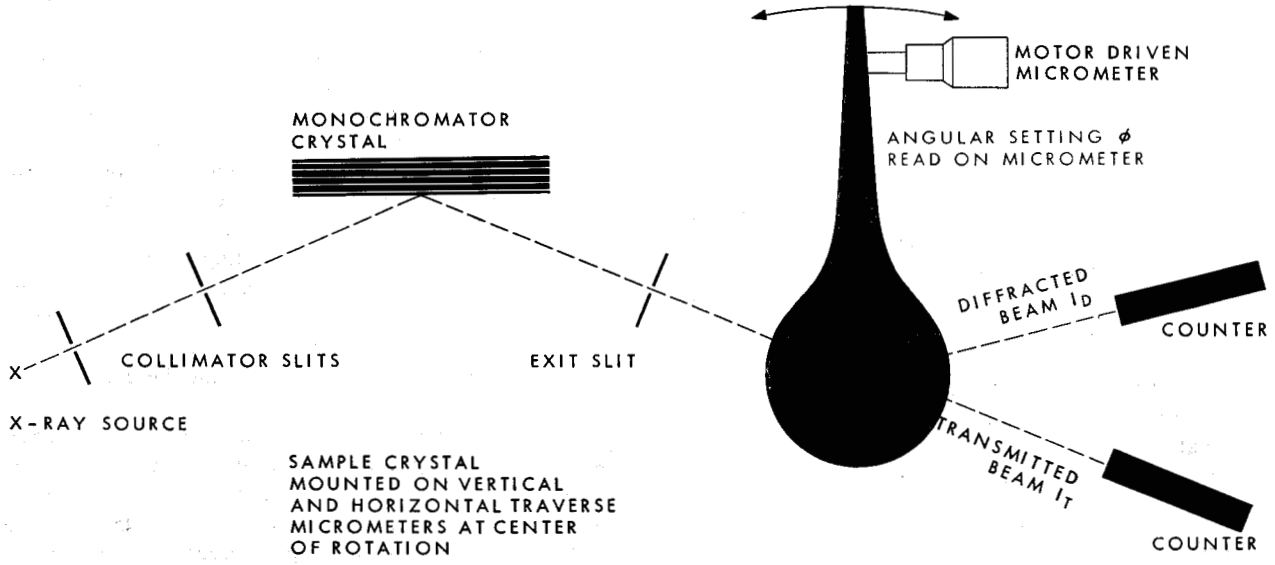

voltage and current on the x-ray tube to see if the ratio I_T/I_0 were higher for the higher voltage settings. Since no effect was found, it was concluded that no significant intensity of higher harmonics was being counted.

The initial samples used for the measurements were cut wedge-shaped, with the diffracting planes perpendicular to the direction of taper of the wedge. The wedges were mounted so that the long dimension of the x-ray beam was parallel to the crystal planes. The crystal translations mentioned above provided the ability to scan along the length of the wedge without changing its angle to the x-ray beam and maintaining the axis of rotation within the crystal. A typical wedge was 20 mm long, 3 mm wide and tapered from a thickness of about 0.5 mm to 1.5 mm.

A study was made of the effects of surface damage due to grinding the sample to shape. It was found that the anomalous transmission measured on a 1-mm sample, ground to shape and lapped with 1200-mesh abrasive to remove all grinding scratches, was only about 5% of the transmission measured after a heavy CP4 etch. (This percentage includes correction for the reduced thickness.) Experimentation showed that if 20 microns or more were removed by etching from the surfaces through which the x-rays pass, there was no reduction of the anomalous transmission by surface damage.

The measurement of I_0 was achieved by using the thin end of the sample crystal wedge as a filter. The x-ray tube was first set at a current and voltage within the regulating range of the x-ray generator and yet at a sufficiently low level that the proportional counter could measure the direct beam from the monochromator. At this setting of current and voltage both the direct beam and the integrated intensity through the thin end of the crystal wedge were measured. The x-ray generator was now set at the usual operating current and voltage, and the integrated intensity was again measured through the same point on the crystal wedge, thus providing a calibrating factor.

In order to use the equations developed above, we must know the μ_0 of single-crystal germanium for the wavelengths of the x-rays to be used. Even though values of μ_0 are to be found in the literature it was felt desirable to measure it directly. For this purpose a slab of germanium single crystal was lapped and etched to a thickness of 0.210 mm. The normal transmission of the monochromatic x-rays was measured through this slab for several different angles of incidence of the x-rays. Since this slab was taken from a good single crystal it was possible to use the anomalous transmission method of determining I_0 as described above. The normal transmissions at the various angular settings were corrected for the cosine of the angle, and the resulting values of I_T/I_0 were averaged to yield $\mu_0 = 326$ per cm for Cu$K\alpha_1$ radiation.

Wedge samples were used to determine the value of $[1-f''_{Ge}(\theta_B)/f''_{Ge}(0°)]$ for the (220) and (400) reflections by the extrapolation method described in the discussion of Eq. (12). The plotting of Eq. (12), as described, requires only that we have measured the anomalous transmission as a function of $\mu_0 t$. Since scanning our wedge-shaped samples provides a variation in t, we can get enough data from one wedge sample to give a complete determination of $[1-f''_{Ge}(\theta_B)/f''_{Ge}(0°)]$ for one reflection.

For higher-order reflections wedge samples were not used, because the reduced anomalous transmission of the higher orders will not allow sufficiently large values of t to be measured to give a good extrapolation to $t=\infty$. To measure the higher-order reflections, samples were prepared in the form of flat discs of uniform thickness and oriented so that the [110] crystallographic direction is perpendicular to the plane of the disc. A disc oriented in this way has the [100], [110] and [112] crystallographic directions at different azimuths in the plane of the disc.

Figure 3 **Schematic arrangement of apparatus for anomalous-transmission measurement.**

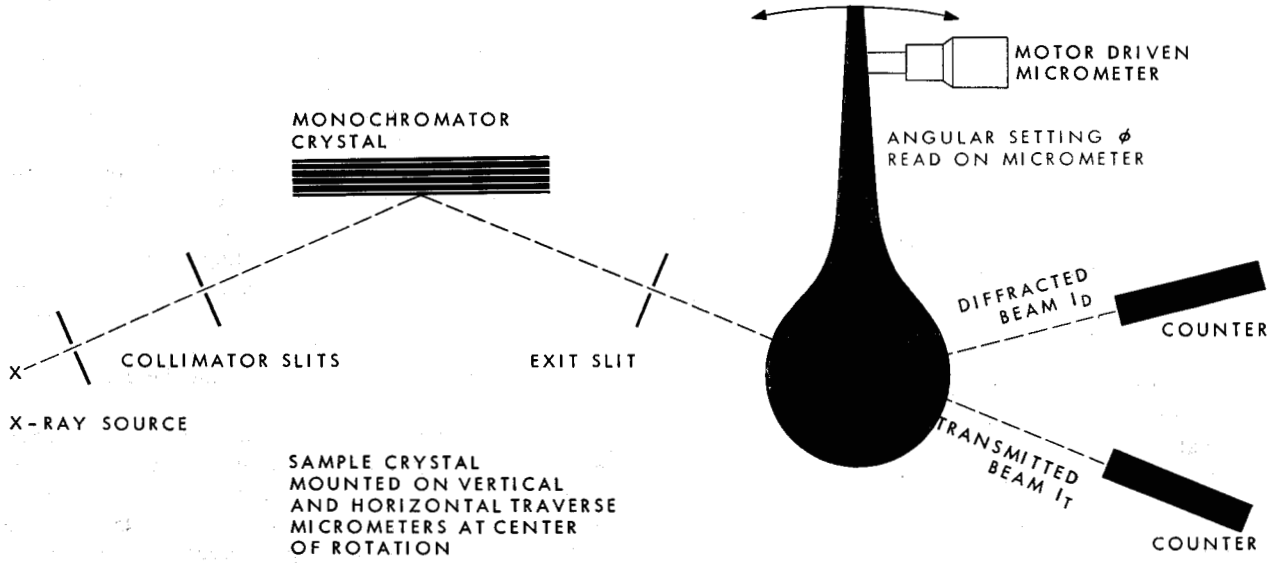

This means that we can measure the (220), (400), (224), and (440) reflections by mounting the disc with its perpendicular in the plane of reflection of the x-rays and selecting different azimuths. In this way we can compare the anomalous transmission intensities of the different reflections at one point in the disc and compute the $[1-f''_{Ge}(\theta_B)/f''_{Ge}(0°)]$ values of the higher orders in terms of the values of this quantity for the lower orders. Formulae for this calculation will be given later.

Results

In Fig. 4 are shown results of measurements made on five samples cut from three different crystals of germanium. The (220) reflection is used and the crystal wedges were cut so that the [110] direction is parallel to the direction of taper of the wedge. Crystal 1 was grown in the [110] direction and Crystals 2 and 3 were grown in the [111] direction. This means that the wedge of Crystal 1 was cut parallel to the axis of growth of the crystal and the wedges cut from Crystals 2 and 3 were cut perpendicular to the axis of growth. All of these crystals were free of dislocation etch pits. Figure 4 is a plot of Eq. (12) and should be a 45° line except for the slight variation introduced by using an assumed value of $f''_{Ge}(\theta_B)/f''_{Ge}(0°)$ in the calculation of the abscissa. In making the plot shown, a preliminary plot was made assuming $f''_{Ge}(\theta_B)/f''_{Ge}(0°)=1.00$. The resulting intercept $[1-f''_{Ge}(\theta_B)/f''_{Ge}(0°)]$ was 0.05, giving a value of $f''_{Ge}(\theta_B)/f''_{Ge}(0°)=0.95$. The final plot Fig. 4 was then made using this value, and the intercept finally becomes $[1-f''_{Ge}(\theta_B)/f''_{Ge}(0°)]=0.047\pm0.002$ for the best straight line through all the points shown.

Brief consideration of the effect of crystal imperfections shows that they should tend to increase this numerical value of the intercept since they would tend to decrease E. A correction for the effect of microstrains will be discussed later. Since a transmission greater than that of of a perfect crystal is very unlikely, we conclude that this value of the intercept is an upper limit.

For higher-order reflections it is easier to compare the transmitted intensities of such reflections with the transmitted intensity of the (220) reflection at a given point in a crystal of uniform thickness, rather than try to measure wedges cut separately for each reflection. We accordingly will derive appropriate comparison formulas.

Remembering that $t=t_0/\cos\theta_B$, and letting $\varepsilon_B=f''_{Ge}(\theta_B)/f''_{Ge}(0°)$, we may rewrite Eq. 12 as:

$$\exp\left[\frac{\mu_0 t_0}{\cos\theta_B}(1-\varepsilon_B)\right]=\frac{I_0 C 4 f_{Ge}}{\omega E_B \sin 2\theta_B}\left(\frac{\pi\cos\theta_B}{8\mu_0 t_0 \varepsilon_B}\right)^{1/2}. \quad (13)$$

We will now calculate $(1-\varepsilon_B)$ in terms of $(1-\varepsilon_{220})$. First taking the ratio of Eq. (13) for $(1-\varepsilon_B)$ to Eq. (13) for $(1-\varepsilon_{220})$, we have:

$$\exp\left[\mu_0 t_0\left(\frac{1-\varepsilon_B}{\cos\theta_B}-\frac{1-\varepsilon_{220}}{\cos\theta_{220}}\right)\right]=\frac{E_{220}\sin 2\theta_{220}(\varepsilon_{220}/\cos\theta_{220})^{1/2}}{E_B \sin 2\theta_B(\varepsilon_B/\cos\theta_B)^{1/2}}. \quad (14)$$

Taking the logarithm and solving for $(1-\varepsilon_B)$, we get:

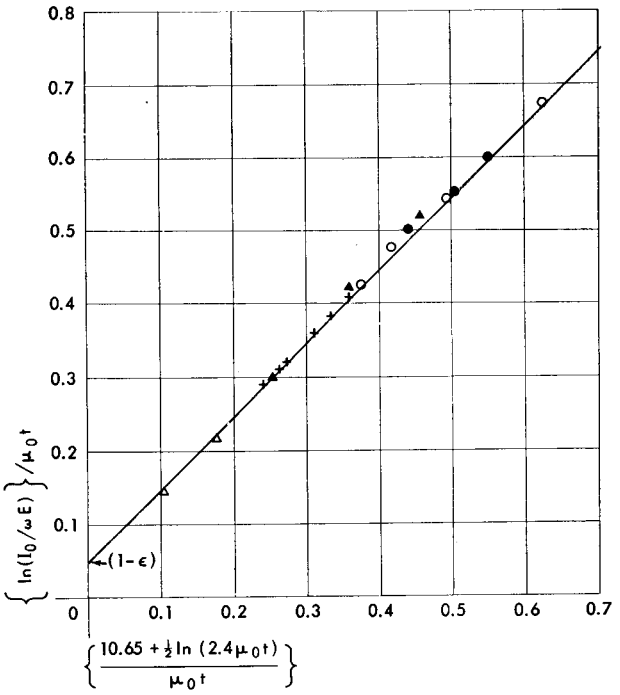

Figure 4 **Plot of Eq. (12) for five wedges cut from three different crystals of germanium. Sample 1 (+) was cut parallel to the axis (110) of Crystal 1; samples 2 (○) and 3 (●) were cut perpendicular to the axis (111) of Crystal 2; and samples 4 (△) and 5 (▲) were cut perpendicular to the axis (111) of Crystal 3.**

$$1-\varepsilon_B=(1-\varepsilon_{220})\frac{\cos\theta_B}{\cos\theta_{220}}+\left[\ln\frac{E_{220}}{E_B}+\ln\frac{\sin 2\theta_{220}}{\sin 2\theta_B}+\frac{1}{2}\ln\frac{\varepsilon_{220}\cos\theta_B}{\varepsilon_B\cos\theta_{220}}\right]\frac{\cos\theta_B}{\mu_0 t_0}. \quad (15)$$

Equation (15) is in a form which makes the calculation of $1-\varepsilon_B$ from the known ε_{220} quite easy. In Table 1 are listed the numerical forms of Eq. (15) ready for the calculation of $1-\varepsilon_B$ for several reflections in germanium, using Cu$K\alpha_1$ radiation. It should be pointed out that Eq. (15) assumes a symmetrical Laue reflection for each of the measured reflections to be compared. If a crystal cut is used in which a nonsymmetrical condition exists,

Table 1 **Equation (15) reduced for use with Cu$K\alpha_1$ radiation.**

Reflection (hkl)	*Comparison with (220) for* $(1-\varepsilon_{220})=0.047$
(400)	$(1-\varepsilon_{400})=0.043+[\ln(E_{220}/E_{400})-\frac{1}{2}\ln\varepsilon_{400}-0.32]/388t_0$
(224)	$(1-\varepsilon_{224})=0.039+[\ln(E_{220}/E_{224})-\frac{1}{2}\ln\varepsilon_{224}-0.46]/435t_0$
(440)	$(1-\varepsilon_{440})=0.033+[\ln(E_{220}/E_{440})-\frac{1}{2}\ln\varepsilon_{440}-0.54]/510t_0$
(444)	$(1-\varepsilon_{444})=0.017+[\ln(E_{220}/E_{444})-\frac{1}{2}\ln\varepsilon_{444}-0.60]/952t_0$

This means that we can measure the (220), (400), (224), and (440) reflections by mounting the disc with its perpendicular in the plane of reflection of the x-rays and selecting different azimuths. In this way we can compare the anomalous transmission intensities of the different reflections at one point in the disc and compute the $[1-f''_{Ge}(\theta_B)/f''_{Ge}(0°)]$ values of the higher orders in terms of the values of this quantity for the lower orders. Formulae for this calculation will be given later.

Results

In Fig. 4 are shown results of measurements made on five samples cut from three different crystals of germanium. The (220) reflection is used and the crystal wedges were cut so that the [110] direction is parallel to the direction of taper of the wedge. Crystal 1 was grown in the [110] direction and Crystals 2 and 3 were grown in the [111] direction. This means that the wedge of Crystal 1 was cut parallel to the axis of growth of the crystal and the wedges cut from Crystals 2 and 3 were cut perpendicular to the axis of growth. All of these crystals were free of dislocation etch pits. Figure 4 is a plot of Eq. (12) and should be a 45° line except for the slight variation introduced by using an assumed value of $f''_{Ge}(\theta_B)/f''_{Ge}(0°)$ in the calculation of the abscissa. In making the plot shown, a preliminary plot was made assuming $f''_{Ge}(\theta_B)/f''_{Ge}(0°)=1.00$. The resulting intercept $[1-f''_{Ge}(\theta_B)/f''_{Ge}(0°)]$ was 0.05, giving a value of $f''_{Ge}(\theta_B)/f''_{Ge}(0°)=0.95$. The final plot Fig. 4 was then made using this value, and the intercept finally becomes $[1-f''_{Ge}(\theta_B)/f''_{Ge}(0°)]=0.047\pm0.002$ for the best straight line through all the points shown.

Brief consideration of the effect of crystal imperfections shows that they should tend to increase this numerical value of the intercept since they would tend to decrease E. A correction for the effect of microstrains will be discussed later. Since a transmission greater than that of of a perfect crystal is very unlikely, we conclude that this value of the intercept is an upper limit.

For higher-order reflections it is easier to compare the transmitted intensities of such reflections with the transmitted intensity of the (220) reflection at a given point in a crystal of uniform thickness, rather than try to measure wedges cut separately for each reflection. We accordingly will derive appropriate comparison formulas.

Remembering that $t=t_0/\cos\theta_B$, and letting $\varepsilon_B=f''_{Ge}(\theta_B)/f''_{Ge}(0°)$, we may rewrite Eq. 12 as:

$$\exp\left[\frac{\mu_0 t_0}{\cos\theta_B}(1-\varepsilon_B)\right]=\frac{I_0 C 4 f_{Ge}}{\omega E_B \sin 2\theta_B}\left(\frac{\pi\cos\theta_B}{8\mu_0 t_0 \varepsilon_B}\right)^{1/2}. \quad (13)$$

We will now calculate $(1-\varepsilon_B)$ in terms of $(1-\varepsilon_{220})$. First taking the ratio of Eq. (13) for $(1-\varepsilon_B)$ to Eq. (13) for $(1-\varepsilon_{220})$, we have:

$$\exp\left[\mu_0 t_0\left(\frac{1-\varepsilon_B}{\cos\theta_B}-\frac{1-\varepsilon_{220}}{\cos\theta_{220}}\right)\right]=\frac{E_{220}\sin 2\theta_{220}(\varepsilon_{220}/\cos\theta_{220})^{1/2}}{E_B \sin 2\theta_B(\varepsilon_B/\cos\theta_B)^{1/2}}. \quad (14)$$

Taking the logarithm and solving for $(1-\varepsilon_B)$, we get:

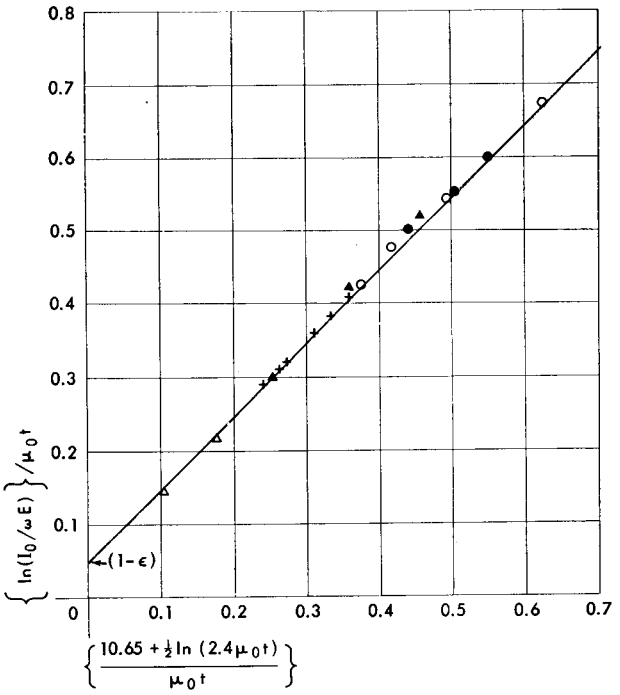

Figure 4 **Plot of Eq. (12) for five wedges cut from three different crystals of germanium. Sample 1 (+) was cut parallel to the axis (110) of Crystal 1; samples 2 (○) and 3 (●) were cut perpendicular to the axis (111) of Crystal 2; and samples 4 (△) and 5 (▲) were cut perpendicular to the axis (111) of Crystal 3.**

$$1-\varepsilon_B=(1-\varepsilon_{220})\frac{\cos\theta_B}{\cos\theta_{220}}+\left[\ln\frac{E_{220}}{E_B}+\ln\frac{\sin 2\theta_{220}}{\sin 2\theta_B}+\frac{1}{2}\ln\frac{\varepsilon_{220}\cos\theta_B}{\varepsilon_B\cos\theta_{220}}\right]\frac{\cos\theta_B}{\mu_0 t_0}. \quad (15)$$

Equation (15) is in a form which makes the calculation of $1-\varepsilon_B$ from the known ε_{220} quite easy. In Table 1 are listed the numerical forms of Eq. (15) ready for the calculation of $1-\varepsilon_B$ for several reflections in germanium, using Cu$K\alpha_1$ radiation. It should be pointed out that Eq. (15) assumes a symmetrical Laue reflection for each of the measured reflections to be compared. If a crystal cut is used in which a nonsymmetrical condition exists,

Table 1 **Equation (15) reduced for use with Cu$K\alpha_1$ radiation.**

Reflection (hkl)	*Comparison with (220) for* $(1-\varepsilon_{220})=0.047$
(400)	$(1-\varepsilon_{400})=0.043+[\ln(E_{220}/E_{400})-\frac{1}{2}\ln\varepsilon_{400}-0.32]/388t_0$
(224)	$(1-\varepsilon_{224})=0.039+[\ln(E_{220}/E_{224})-\frac{1}{2}\ln\varepsilon_{224}-0.46]/435t_0$
(440)	$(1-\varepsilon_{440})=0.033+[\ln(E_{220}/E_{440})-\frac{1}{2}\ln\varepsilon_{440}-0.54]/510t_0$
(444)	$(1-\varepsilon_{444})=0.017+[\ln(E_{220}/E_{444})-\frac{1}{2}\ln\varepsilon_{444}-0.60]/952t_0$

Table 2 **$[1-f''_{Ge}(\theta_B)/f''_{Ge}(0°)]$ for several reflections in germanium using Cu$K\alpha_1$ radiation.**

hkl	θ_B	$[1-f''_{Ge}(\theta_B)/f''_{Ge}(0°)]$	$f''_{Ge}(\theta_B)/f''_{Ge}(0°)$
220	22.6°	0.047	0.953
400	33.1°	0.10	0.90
224	41.7°	0.15	0.85
440	50.4°	0.22	0.78

Table 3 **$[1-f''_{Ge}(\theta_B)/f''_{Ge}(0°)]$ for several reflections in germanium corrected for strain in the sample. (Cu$K\alpha_1$ radiation.)**

hkl	θ_B	$[1-f''_{Ge}(\theta_B)/f''_{Ge}(0°)]$	$f''_{Ge}(\theta_B)/f''_{Ge}(0°)$
220	22.6°	0.039	0.961
400	33.1°	0.085	0.915
224	41.7°	0.130	0.870
440	50.4°	0.185	0.815

special comparison equations must be derived using both sets of direction cosines throughout. As pointed out previously, all of the reflections listed in Table 1 can be obtained in the symmetrical Laue condition from a crystal slab cut so that the [110] direction is perpendicular to the plane of the slab.

Examination of Table 1 shows that relatively thin crystal slabs must be used for measuring the higher-order reflections. For example, a 1 mm slab will show $E_{220}/E_{440}=20{,}000$. Because of this it is usually better to use more than one crystal slab to measure a large range of reflections.

In Table 2 is given the results for several reflections measured by comparison with the (220) reflection. The value of $(1-\varepsilon_{220})$ was determined by the extrapolation plot of Eq. (12) described above.

These results were obtained on crystals which showed no dislocation etch pits but which showed considerable evidence of the presence of microstrain.[11] The effect of the microstrain on the measured transmitted intensity can be calculated from the variation of transmitted intensity as the sample is bent elastically. From Reference 11 we have the relation:

$$\alpha=(T_0/E_0)a\,, \tag{16}$$

where

$a = 6.2 \times 10^4$ cm$^{-1/2}$, and is evaluated from the theory of a bent crystal.

α is the measured slope of an experimental curve of $(\ln T_0/T)^{1/2}$ *vs* $\Sigma\sqrt{t}$.

E_0 is the transmitted intensity of a perfect unbent crystal.

T_0 is the transmitted intensity of the imperfect unbent crystal.

T is the transmission of the imperfect crystal under the conditions of an elastic bend of Σ units of strain in the extreme fiber.

t is the thickness of the bent crystal.

Since it is necessary to have a sample of uniform thickness for the measurements on a bent crystal, it was not possible to make the determination of (T_0/E_0) on the identical crystals used in the measurements of $[1-f''_{Ge}(\theta_B)/f''_{Ge}(0°)]$. A crystal bar cut from the same ingot used for obtaining most of the above results was used for the bending measurements, and its exact relation to the other samples is shown in Fig. 5. The wedge-shaped sample ① shown in Fig. 5 is also the sample 1(+) of Fig. 4. This sample was cut adjacent to the central axis of the crystal ingot. Sample ④ is a 1-mm thick bending specimen used to determine the (T_0/E_0) ratio for material near the axis of the ingot. Samples ② and ③ are transverse discs used to measure the comparative transmissions of the various orders reported above. (These are not the samples 2(○) and 3(●) of Fig. 4.)

In Fig. 6 is shown the results of the bending measurements on sample ④ of Figure 5. From the slope of this curve we find $(T_0/E_0)=0.57$. Correcting the ωE readings of sample ① by a factor of $1/57=1.75$, we find a corrected value of 0.039 for the $[1-f''_{Ge}(\theta_B)/f''_{Ge}(0°)]$ intercept. Making a similar correction for the higher order reflections we get the corrected results shown in Table 3.

Conclusions

The results given above show that it is possible to measure directly the imaginary part of the atomic scattering factor as a function of the order of reflection and thus as a function of angle. It could similarly be measured for the same

Figure 5 **Location of samples in germanium ingot. Samples ①, ② and ③ were used for $f''_{Ge}(\theta_B)/f''_{Ge}(0°)$ determinations and samples ④ and ⑤ were used for bending determinations of T_0/E_0.**

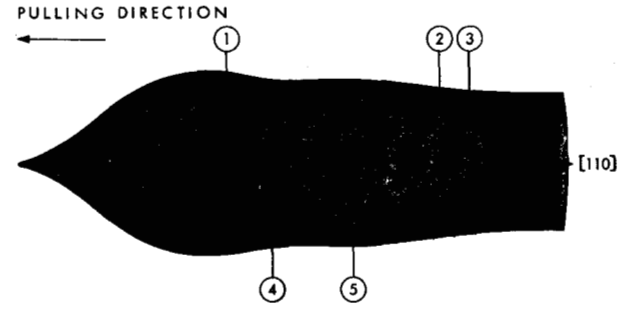

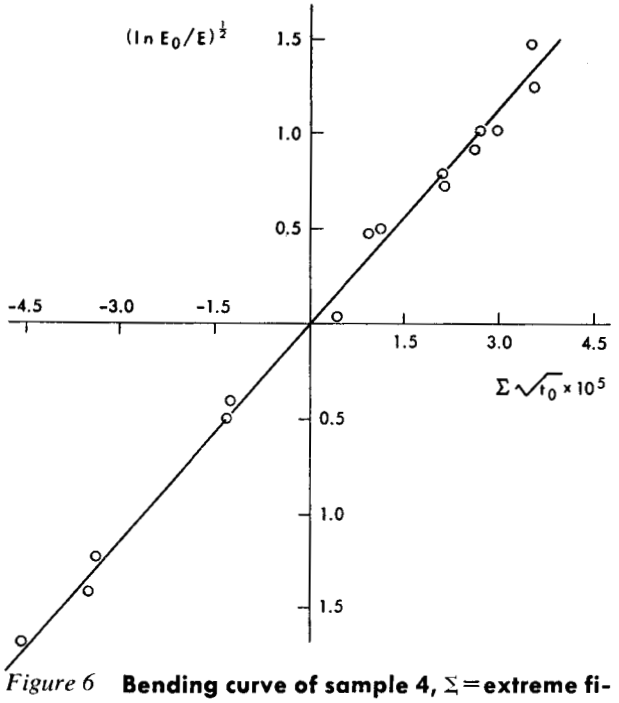

Figure 6 **Bending curve of sample 4, Σ = extreme fiber strain, E_0 = transmission for zero strain.**

reflection as a function of wavelength. Such a measurement would vary the energy difference between the x-ray photons and the L absorption edge as well as the angle. It seems reasonable that such measurements should be made in order to collect enough data to calculate the electron-density function of the L electrons in germanium. Even more interesting results might be obtained in silicon if sufficiently perfect crystals are available.

It should be pointed out that the only other way of finding the imaginary part of the atomic scattering factor is through the well-known Hönl corrections.[12] These corrections are not capable of yielding values comparable in accuracy to the results reported here.

The accuracy of the results reported here depends upon the accuracy of the corrections for strain in the sample. Since the strain correction used here is only a first-order correction depending upon strain which shows a monotonic variation of lattice spacing through the thickness of the crystal, we can conclude that all of the corrected $(1-\varepsilon)$ values are, if anything, too large. It is difficult to estimate the size of the second-order corrections due to strain, but they probably only affect the $(1-\varepsilon)$ values to about 10% at the most and indeed may actually be negligible. It seems reasonable that the accuracy of these measurements could be improved if the determination of $(1-\varepsilon)$ and of (T_0/E_0) were made at a single point on the same crystal. This would ensure that the microstrain distribution would be the same for all measurements. Such a measurement could be accomplished by starting with a thick crystal bar and slowly reducing its thickness to obtain various values of $\mu_0 t$. Since the thickness would be uniform for each set of measurements, it would be possible to make both a bending experiment and a transmitted-intensity measurement at each thickness.

It should be pointed out that it is impractical to measure I_T/I_0 directly as a function of y in Eq. (1) in order to determine ε better. This is true because microstrain shows up in a change of intensity rather than a line broadening for anomalous transmission in thick crystals ($\mu_0 t > 20$). The results of Schwarz and Rogosa[7] are for relatively thin crystals where $\mu_0 t < 10$. In our case, the theoretical line width would be about 4 seconds of arc and quite insensitive to microstrain.

Another interesting line of investigation which suggests itself is the measurement of the temperature variation of the anomalous transmission as a function of the order of the reflection. Such a measurement should yield considerable information about the lattice vibration amplitudes in the various directions.

Acknowledgments

The work reported here was carried out while the author was a visitor at the Philips Research Laboratories, Eindhoven. The cooperation of the management of this laboratory is most gratefully acknowledged. In particular, the author wishes to express his gratitude to Dr. P. B. Braun for making available the necessary x-ray equipment and for innumerable helpful discussions, to Dr. Ir. B. Okkerse for providing the dislocation-free crystals used, to Dr. D. Polder, Ir. P. Penning, Dr. J. Hornstra and Dr. H. van Bueren for many helpful discussions.

References

1. G. Borrmann, *Physik Z.* **43,** 157 (1941) and *Physik Z.* **127,** 297 (1950).
2. H. N. Campbell, *Acta Cryst.* **4,** 180 (1951).
3. P. B. Hirsch, *Acta Cryst.* **5,** 176 (1952).
4. M. von Laue, *Acta Cryst.* **5,** 619 (1952).
5. W. H. Zachariasen, *Proc. Nat. Acad. Sci.* (U. S.) **38,** 378 (1952).
6. N. Kato, *J. Phys. Soc. Jap.* **7,** 397 (1952).
7. G. Schwarz and G. L. Rogosa, *Phys. Rev.* **95,** 950 (1954).
8. L. P. Hunter, *Konikl Nederl. Akademie van Wetenschappen* **61,** series **B,** 214 (1958).
9. A. G. Tweet, *Bull. Am. Phys. Soc.* **3,** No. 4, Abstract **F9** (1958).
10. W. Bontinck and S. Amelinckx, *Phil. Mag.* **2,** 94 (1957).
11. L. P. Hunter, *J. Appl. Phys.* (to be published in June 1959).
12. R. W. James, *The Optical Principles of the Diffraction of X-Rays,* Chapter IV, G. Bell and Sons, Ltd., London, 1950.

Revised manuscript received December 22, 1958